Strength of the resonance of the $^{13}C(\alpha, n)^{16}O$ reaction at $E_\alpha = 1055.63$ keV

L. H. Ru,[1,2] D. H. Xie,[3] T. Y. Jiao,[1,2] Z. An,[3] F. Bai,[3] J. W. Cai,[1,2] X. Fang,[4] Y. H. Fan,[1,2] Y. X. Fan,[3] B. S. Gao,[1,2] Y. Z. Li,[1,2] W. P. Lin,[3,*] G. Liu,[3] L. Ma,[3] H. J. Ong,[1,2,5,6,7] X. D. Tang,[1,2,5,†] P. Wang,[3] and X. Zhang[3]

[1]*Institute of Modern Physics, Chinese Academy of Sciences, Lanzhou 730000, China*
[2]*School of Nuclear Science and Technology, University of Chinese Academy of Sciences, Beijing 100049, China*
[3]*Key Laboratory of Radiation Physics and Technology of the Ministry of Education, Institute of Nuclear Science and Technology, Sichuan University, Chengdu 610064, China*
[4]*Sino-French Institute of Nuclear Engineering and Technology, Sun Yat-sen University, Zhuhai 519082, China*
[5]*Joint Department for Nuclear Physics, Lanzhou University and Institute of Modern Physics, Chinese Academy of Sciences, Lanzhou 730000, China*
[6]*Research Center for Nuclear Physics, Osaka University, Ibaraki, Osaka 567-0047, Japan*
[7]*RIKEN Nishina Center, Wako, Saitama 351-0198, Japan*

(Received 13 January 2023; accepted 23 May 2023; published 7 June 2023)

The strength of the narrow resonance of the $^{13}C(\alpha, n)^{16}O$ reaction at $E_\alpha = 1055.63$ keV is determined to be $16.9 \pm 0.4(\text{stat}) \pm 1.7(\text{sys})$ eV. The resonance strength and the cross section in the vicinity of the resonance are used to reconcile inconsistencies of past measurements. Our normalization factors agree with the recommendation of the ENDF/B-VIII.0 evaluation and the CIELO project. The sum of the resonance strengths of the two narrow resonances around $E_\alpha = 1336$ keV is also determined to be $57.3 \pm 4.8(\text{stat}) \pm 5.7(\text{sys})$ eV.

DOI: 10.1103/PhysRevC.107.065803

I. INTRODUCTION

The $^{13}C(\alpha, n)^{16}O$ reaction rate is a fundamental ingredient of the *s* and *i* processes in nuclear astrophysics [1]. Its cross section at stellar energies determines the neutron density and the final isotopic production in the stellar models. Precise reaction cross section is needed at the Gamow energies of $E_{\text{c.m.}} = 0.15$ to 0.30 MeV for the *s* process, and 0.20 to 0.54 MeV for the *i* process. Considerable efforts have been devoted to pushing the direct measurement of the $^{13}C(\alpha, n)^{16}O$ reaction cross section down to the stellar energies where cross sections become extremely small. Although direct measurements to date cover nearly the entire Gamow window of the *i* process with uncertainties better than 15%, they are restricted to energies above $E_{\text{c.m.}} = 0.23$ MeV ($E_\alpha = 0.3$ MeV) by the exponentially vanishing reaction yield at lower energies. The extrapolation toward the *s*-process Gamow window is therefore inevitable. The extrapolation accuracy, however, is limited by the large discrepancies among those measurements [2]. The ≈40% discrepancy of the absolute normalization between the measurement by Harissopulos *et al.* [3] and the other measurements, such as the measurement by Heil *et al.* [4] at $E_\alpha < 0.9$ MeV and that of Drotleff *et al.* [5] in the range of $E_\alpha < 1.39$ MeV, leads to a nearly 50% difference in the reaction rate. A consistent measurement was performed in the range of $E_{\text{c.m.}} = 0.24$ to 1.9 MeV ($E_\alpha = 0.314$ to 2.5 MeV), confirming the measurements of Heil *et al.* and Drotleff *et al.* while being in disagreement with that of Harissopulos *et al.* [1].

The $^{13}C(\alpha, n)^{16}O$ reaction is a dominant source of background in the geoneutrino experiments. It contributes a number of fake events which are comparable to those expected from geoneutrinos. A 10% uncertainty in the $^{13}C(\alpha, n)^{16}O$ reaction cross section in the range of $E_\alpha = 1.0$ to 5.4 MeV is essential to the success of the geoneutrino experiments [3,6].

Oxygen is an important element for criticality safety applications in which large quantities of fissile oxide configurations are present. The $^{16}O(n, \alpha)^{13}C$ reaction is one of the important reactions. Its evaluation at energies below $E_\alpha < 5.1$ MeV, however, heavily depends on the measured $^{13}C(\alpha, n)^{16}O$ cross sections reported by Bair and Haas [7] and Harissopulos *et al.* [3]. The discrepancy between the absolute normalizations of the two data sets leads to significant ambiguity in the $^{16}O(n, \alpha)^{13}C$ cross section, attracting considerable interest and debates [8].

Correct neutron detection efficiency is crucial to obtain a precise $^{13}C(\alpha, n)^{16}O$ reaction cross section. The strength of the narrow resonance at $E_\alpha = 1055.63$ keV [9] is a standard for the efficiency calibration of neutron detector arrays. In early measurements, standard neutron sources, such as Sb-Be [7] and ^{252}Cf [3,10], were used to calibrate the detection efficiency. Efficiency curves were calculated using analytic solutions or simulations and extrapolated to the uncovered energy range. Later, semimonoenergetic neutrons produced by the $^{51}V(p, n)^{51}Cr$ and $^{13}C(\alpha, n)^{16}O$ reactions were used. While the former reaction only covers energies up to about $E_n = 0.7$ MeV, the neutrons coming from the narrow resonances of $^{13}C(\alpha, n)^{16}O$ at $E_\alpha = 1055.63$ keV span the energy

*linwp1204@scu.edu.cn
†xtang@impcas.ac.cn

range of 2.4 to 3.2 MeV. Using the measured resonance strength [10], the detection efficiencies of neutron detector arrays, such as NERO [11] and HeBGB [12], were determined at the energies around 2.8 MeV by normalizing their result to the predicted yield based on the measured resonance strength. Besides the neutron detection efficiency calibration, the strength of the narrow resonance of the $^{13}C(\alpha, n)^{16}O$ was also used to analyze the ^{13}C impurities in targets. A precise resonance strength is of fundamental importance in these applications.

In this paper, we report a measurement of the strength of the $E_\alpha = 1055.63$ keV resonance using a thick target method. The resonance parameters extracted from our measurement are compared with the ones obtained from the previous measurements. Using the resonance strength and the consistent cross section measurement in the vicinity of the resonance, we propose a new set of normalization factors for some of the past measurements.

II. EXPERIMENTAL SETUP

The current data are a subset of the data in Ref. [1]. The measurement was performed with a $^4He^+$ beam delivered by the 3 MV Tandetron accelerator at Sichuan University (SCU) [13]. A 2-mm-thick enriched ^{13}C target with a purity of 97% (mass fraction) was used. The target was mounted on a water-cooled copper backing to control the target temperature. A copper cold trap was installed in front of the target to reduce the natural carbon buildup. A suppressor with a negative voltage of not less than 1000 V was placed in front of the target to suppress the secondary electrons. Neutrons were detected by a low background neutron detector array consisting of 24 cylindrical ^{3}He-filled proportional counters. The detection efficiency was calibrated with the $^{51}V(p, n)^{51}Cr$ reaction with neutron energies up to 1 MeV. A GEANT4 simulation was used to extend the efficiency curve towards higher energies. A detailed description of the neutron detector array is given in Ref. [14].

III. THICK TARGET YIELD

The resonant cross section $\sigma_r(E_{c.m.})$ is calculated using

$$\sigma_r(E_{c.m.}) = \frac{1}{4\pi}\lambda^2\frac{(\omega\gamma)\Gamma}{(E_{c.m.} - E_{R,c.m.})^2 + (\Gamma/2)^2}. \quad (1)$$

in which $E_{c.m.}$, $E_{R,c.m.}$, $\omega\gamma$, and Γ represent the energy, the resonance energy, the resonance strength and the resonance width in the center-of-mass frame, respectively. The thick target yield for an incident α particle is obtained using

$$Y(E_0) = fN_v\int_0^{E_0}[\sigma_r(E) + \sigma_{nr}(E)]\varepsilon(E)\frac{dE}{S(E)}. \quad (2)$$

Here σ_{nr} is the nonresonant component of the cross section. N_v is the number density of the atoms in the target. E and $S(E)$ are the energy in the laboratory frame and the stopping power, respectively. $\varepsilon(E)$ is the detection efficiency, f is the atomic percentage of ^{13}C in the target, and E_0 is the incident energy of the α particle in the laboratory frame.

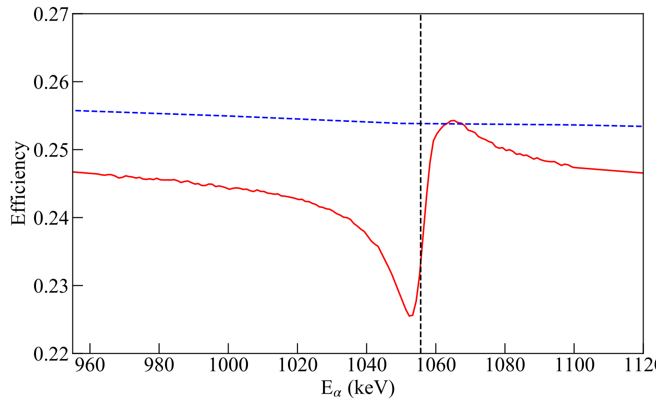

FIG. 1. The detection efficiency simulated for the $^{13}C(\alpha, n)^{16}O$ reaction. E_α is the α-particle energy in the laboratory frame. The results simulated with the ENDF compilation and isotropic angular distribution are shown as the red solid and the blue dashed lines, respectively. The vertical line indicates the resonant energy.

The resonance strength $\omega\gamma$ is obtained by integrating the resonant cross section σ_r from 0 to infinity:

$$\omega\gamma = \frac{2}{\lambda_R^2}\frac{m(^{13}C)}{m(^{13}C) + m(^4He)}\int\sigma_r(E)dE. \quad (3)$$

λ_R is the wavelength calculated at the resonant energy in the center-of-mass frame. $m(^{13}C) = 13.003$ u and $m(^4He) = 4.002$ u. If one assumes a constant detection efficiency, $\varepsilon(E)$, and a constant stopping power, $S(E)$, in the energy range of narrow resonance, $\omega\gamma$ and $\sigma_R\Gamma$ can be obtained from Y_{max}, the maximum thick target yield of narrow resonance, using

$$\omega\gamma = \frac{2Y_{max}S(E_R)}{f\lambda_R^2N_v\varepsilon(E_R)}\frac{m(^{13}C)}{m(^{13}C) + m(^4He)}, \quad (4)$$

$$\omega\gamma = \frac{\sigma_R\Gamma}{4\pi\lambda_R^2}. \quad (5)$$

E_R is the resonant energy in the laboratory frame.

A recent study indicates that the assumption of a constant efficiency is not valid in the vicinity of the narrow resonance if the detection efficiency of the neutron detector array depends on the angular distribution [14]. The presence of narrow resonance leads to a dramatic change in the angular distribution according to the ENDF compilation [15]. For the detector array used in this work, the simulated efficiency based on the compiled angular distribution exhibits a rapid change as the energy varies within the energy range of narrow resonance. Compared to the efficiency simulated with an isotropic angular distribution in the center-of-mass frame, the efficiency simulated with the ENDF compilation is lower than the nominal efficiency with a maximum deviation of 11% (see Fig. 1). In this work, we choose to fit the thick target yield using Eq. (2) and the simulated efficiency based on the ENDF compilation.

IV. RESULT AND DISCUSSION

The measured thick target yield around the narrow resonance at $E_\alpha = 1055.63$ keV is shown together with the best-fit

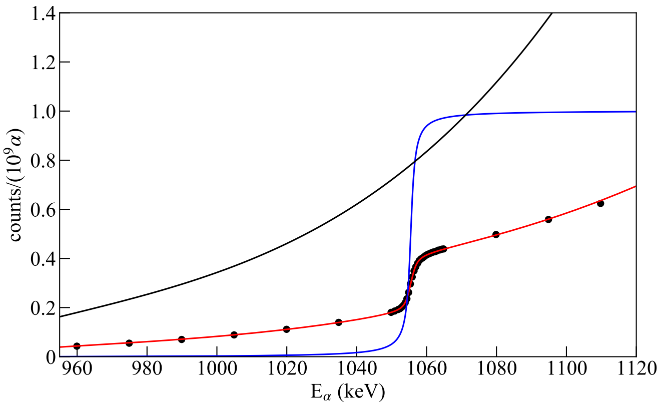

FIG. 2. Measured (black points) and fitted (red line) thick target yield near the $E_\alpha = 1055$ keV resonance. The ENDF angular distribution is used to obtain the best fit. The thick target yields of the resonant and nonresonant components are calculated with the conditions of a pure ^{13}C sample and a detection efficiency of 100%, and shown as blue and black lines, respectively.

yield in Fig. 2. In the fitting, the non-resonant component of the cross section (σ_{nr}) is assumed to be a third-order polynomial in the range of $0.9 < E < 1.14$ MeV with four free parameters. At lower energies, the cross section determined by the R-matrix fit was used [1]. The lower limit of the integration in Eq. (2) is set to be 0.5 MeV in the laboratory frame since the contribution of the lower energy part is negligible. The product of cross section and efficiency in the integrand of Eq. (2) is convoluted by a Gaussian distribution to take the beam energy spread into account. Both the resonance energy in the laboratory frame (E_R) and beam energy spread in the center-of-mass frame (Δ) are treated as free parameters. The resonance width (Γ) is fixed to 1.38 keV in the center-of-mass frame according to the NNDC recommendation [9]. The parameters of the fitting results are listed in Table I. Two different efficiencies, calculated respectively with the ENDF angular distribution and isotropic angular distribution, are used separately to test the effect of the angular distribution. The efficiency curve obtained with the ENDF angular distribution is shifted by 2.29 keV to match the resonant cross section in the present work. The best fit is achieved by using the ENDF angular distribution with a reduced χ^2 of 1.68. The reduced χ^2 increases to 2.61 if an isotropic angular distribution in the center-of-mass frame is used in the fitting. The resonance strengths ($\omega\gamma$) obtained with these two different angular distributions differ from each other by 10%. The dependences of the reduced χ^2

TABLE I. $E_\alpha = 1055.63$ keV resonance parameters of $^{13}C(\alpha, n)^{16}O$.

Ang. dist.	$E_\alpha(E_R)$ (keV)	Δ (keV)	$\omega\gamma$[a] (eV)	$\sigma_{nr}(E_R)$[a] (mb)	χ^2
ENDF	1055.55 ± 0.08	0.73 ± 0.21	16.9 ± 0.4	410 ± 25	1.68
Isotropic	1055.60 ± 0.08	0.72 ± 0.21	15.5 ± 0.4	394 ± 24	2.61

[a]Systematic uncertainty of 10% is not included.

TABLE II. Resonance strength and the thick target yield of the $E_\alpha = 1055.63$ keV resonance.

Reference	$\omega\gamma/eV$	Y_{max} ($n/\mu C$)[a]
This work	16.9 ± 0.4[b]	6460 ± 152[c]
Bair *et al.*	12.9 ± 0.6[d]	4475 ± 223
Brune *et al.*	11.9 ± 0.4[e]	4410 ± 170
Harissopulos *et al.*	12.1 ± 0.6	

[a]Calculated for a pure ^{13}C target.
[b]Systematic uncertainty (10%) is not included.
[c]Systematic uncertainty (8.6%) is not included.
[d]Derived using $S(E) = 39.2/(10^{15}$ atoms/cm^2) [7].
[e]Derived using $S(E) = 36.9/(10^{15}$ atoms/cm^2) [16].

and σ_{nr} on the choice of angular distribution demonstrate the importance of using the realistic angular distribution.

Systematic uncertainty of the resonance strength ($\omega\gamma$) and the nonresonant cross section [$\sigma_{nr}(E_R)$] is estimated to be 10%, which includes contributions from the beam current integration (5%), detection efficiency (7%) [14], and stopping power (5%).

The nonresonant cross section at the resonant energy, $\sigma_{nr}(E_R)$, is an important normalization factor in the analysis of Brune *et al.* [10]. In their work, the recommended $\sigma_{nr}(E_R)$ is 308 ± 15 mb. Our result is 410 ± 25 mb, about 33% higher than the value used in Ref. [10]. Hence, their recommended resonance strength $\omega\gamma$ should increase from 11.9(6) to 15.8(18) eV, agreeing well with our result shown in Table I.

The maximum thick target yield of the narrow resonance (Y_{max}) is determined to be 6460 ± 152 n/(μC) with the conditions of a pure ^{13}C sample and a detection efficiency of 100%. For comparison, the thick target yields obtained in this work and previous works are shown in Table II. The systematic uncertainty is 8.6%, including the contributions from the beam current integration (5%) and detection efficiency (7%) [14]. As Y_{max} is derived from our measured thick target yield, there is no dependence on the stopping power. Our yield is more than 30% higher than those of Bair *et al.* and Brune *et al.*

The stopping power $\frac{S(E)}{N_v} = \frac{dE}{N_v dx}$ of the α particle in the carbon target is needed to convert the observed thick target yield (Y_{max}) to the resonance strength ($\omega\gamma$). But the recommended stopping power varied with time and caused the discrepancies in the extracted $\omega\gamma$. At the resonance energy $E_\alpha = 1055.63$ keV, Bair *et al.* used 39.2 eV/(10^{15} atoms/cm^2). This number was updated to be 36.9 eV/(10^{15} atoms/cm^2) in the later work by Brune *et al.* The current version of SRIM [17] recommended 35.7 eV/(10^{15} atoms/cm^2), which corresponds to 1789 MeV/(g/cm^2) for a natural carbon target and 1653 MeV/(g/cm^2) for a pure ^{13}C target, due to the different atomic masses of the carbon isotopes. The ASTAR database [18] suggests two different stopping powers, 1863 MeV/(g/cm^2) for graphite and 1774 MeV(g/cm^2) for amorphous carbon. The comparison of the stopping powers is shown in Fig. 3. In this work, we use the SRIM recommendation to convert the thick target yield to $\omega\gamma$. The systematic uncertainty of the stopping power is estimated as 5% by taking

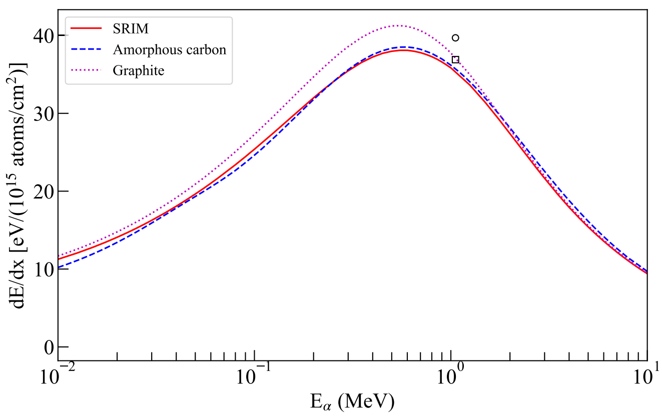

FIG. 3. Comparison of the stopping powers. The stopping powers calculated with ASTAR [18] are represented by the dotted and dashed-dotted lines. The solid line represents the one calculated with SRIM [17]. The stopping powers used by Bair *et al.* [7] and Brune *et al.* [16] are labeled as open circles and open squares, respectively.

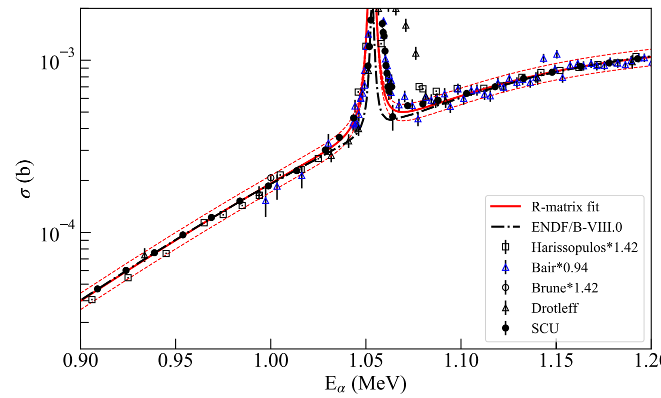

FIG. 4. The cross sections normalized using the factors obtained by this work. The dotted lines are the upper and lower limits including the 10% systematic uncertainty. The broader distribution at the narrow resonance reported by Drotleff *et al.* [5] is a result of target thickness effect.

the difference of the stopping powers in two different carbon materials at the resonance energy.

The resonance strength $\omega\gamma$ obtained with the thick target yield is shown in Table II together with the results from the other works. By using our $\omega\gamma$ as the nominal standard, the normalization factors are determined for the measurements performed by Bair *et al.*, Brune *et al.,* and Harissopulos *et al.*, respectively. The normalization factors are determined as 1.05(5) for Bair's measurement, 1.42(6) for Brune's measurement and 1.40(8) for Harissopulos's measurement. These factors are listed in Table III together with the other recommended normalization factors [15,19]. The normalization coefficient for the data of Bair *et al.* is the ratio of the value from this work to the corresponding Bair *et al.* value reported in Table II, multiplied by a factor of 0.8 (16.9/12.9×0.8). The additional factor of 0.8 is based on the recommendation of normalizing the thin target data in the range of $2 < E_\alpha < 5.3$ MeV to the thick target yield measured with the same setup [7,20].

The cross sections in the range of $E_\alpha = 1.1$ to 1.2 MeV are also used to determine the normalization factors. The results are shown in Fig. 4. The cross section data of SCU and the corresponding R-matrix fit are taken from Ref. [1]. The SCU cross section was determined with the thick target method using the same setup as in this work. Therefore, the R-matrix fit to the SCU cross section is used as the standard for normalization. In the range of $E_\alpha = 1.1$ to 1.2 MeV, the best fits provide a normalization factor of 0.94(1) for Bair's measurement and a normalization factor of 1.42(1) for Harissopulos's measurement. These factors are also listed in Table III. We notice that the difference of two normalization factors for the measurement of Bair and Haas is 0.11(5), nearly 2σ above zero, while two normalization factors work out well for the measurement of Harissopulos *et al.*. As our determination of the first normalization factor relies on the reported resonance strength and normalization factor of the thin target measurement in Ref. [7], some improvement may be needed in these inputs.

TABLE III. Comparisons of the normalization factors.

Measurements	CIELO	Pigni	Norm1[a]	Norm2[b]
Bair *et al.*	0.95	0.80	1.05(5)[c]	0.94(1)
Harissopulos *et al.*	1.36	1.15	1.40(8)	1.42(1)
Brune *et al.*			1.42(6)	

[a]Normalization based on the resonance strength. Systematic uncertainty (10%) is not included.
[b]Normalization based on the cross sections in the range of $E_\alpha = 1.1$ to 1.2 MeV. Systematic uncertainty (10%) is not included.
[c]Additional factor of 0.8, based on the recommendation of normalizing the thin target data in the range of $2 < E_\alpha < 5.3$ MeV to the thick target yield measured with the same setup [7,20], is applied to the ratio of the resonance strengths.

Brune and Kavanagh reported a cross section measurement at $E_\alpha = 1$ MeV [16]. Using our recommended normalization based on the resonance strengths in Table II, the normalized cross section agrees well with other results in Fig. 4 by including the 10% systematic uncertainty.

The ENDF/B-VIII.0 evaluation [15] and the CIELO project [8] recommended a normalization factor of 0.95 for Bair and Hass's measurement based on the unitarity imposed by an R-matrix description. The recommendation was confirmed by comparing the scaled cross section of the reverse reaction, $^{16}O(n,\alpha)^{13}C$ with the measurements and evaluation done at JRC-Geel by Giorginis [15]. The CIELO project recommends a normalization factor of 1.36 for Harissopulos's measurement based on their re-analysis of the target thickness [8]. Our result agrees well with the recommendation of the ENDF/B-VIII.0 evaluation and the CIELO project.

Macklin and Gibbons measured the natural carbon thick target yield using the same detector as Bair and Haas used [21] in the range of $E_\alpha = 2$ to 10.5 MeV. Later, Bair corrected this thick target yield by a factor of 1/20 to account for the charge state of the beam particle and an error in the decimal point [20]. Using the corrected thick target yield, Pigni and Croft determined the normalization factors to be 0.8 for Bair's measurement and 1.15 for Harissopulos's measurement [19], about 15% lower than the normalization factors discussed above. They proposed to revise the normalization factors in the future ENDF evaluation. As we show in Table II, the thick target yield measured by Bair and Haas is about 30% lower than our measurement. Assuming the normalization factor does not depend on energy, the recommended normalization factors should be 1.13 for Bair and 1.62 for Harissopulos. Considering our 10% systematic uncertainty, the revised factors is more than 1σ higher than our recommended factors listed in Table III. A measurement of the thick target yield in the range of $E_\alpha = 1$ to few MeV is useful to check the consistency of the normalization factors.

The discrepancies in the normalization factors for various measurements likely arise from the different ways of calibrating the efficiency curve. Both Brune *et al.* and Harissopulos *et al.* calibrated their detector arrays using a ^{252}Cf source. The efficiency of the graphite sphere detector used by Bair was calibrated using a Sb-Be source which emits neutrons with an energy of 0.024 MeV. The detection efficiency used in this work was calibrated using the semimonoenergetic neutrons from $^{51}\mathrm{V}(p,n)^{51}\mathrm{Cr}$ with energies up to 0.7 MeV. The neutron energy is extended to 1 MeV by including the contribution of the excited state [14]. Using a similar method, the LUNA Collaboration and Heil also calibrated their detection efficiency. As shown in Ref. [1], their measured $^{13}\mathrm{C}(\alpha,n)^{16}\mathrm{O}$ cross sections agree with our measurement within 15% in the overlapped energy ranges of $E_\alpha < 0.8$ MeV.

We note that there are some differences in the energy dependences among the different data sets shown in Fig. 4, indicating that the normalization factors vary with energy. As demonstrated in Fig. 4, at energies below $E_\alpha = 1$ MeV, the normalized cross section measurements of Harrissopulos [3] and Bair [7] are about 10% lower than the *R*-matrix fit, whereas the measurement of Drotleff *et al.* still agrees well with the *R*-matrix fit. The energy of the neutron from $^{13}\mathrm{C}(\alpha,n)^{16}\mathrm{O}$ increases from ≈2.1 MeV with a beam energy of 0.3 MeV to ≈6.9 MeV with a beam energy of 5 MeV. Most neutron detectors suffer from the undesirable attribute of the falling detection efficiency for high-energy neutrons. One has to rely heavily on the simulation to determine the energy dependence of the efficiency curve at such high energies. We estimate the systematic uncertainty of the detection efficiency to be 7% [14]. The efficiency of the graphite sphere detector used in Bair's measurement drops by about 10% when E_α changes from 0.3 to 5 MeV [22]. However, the energy dependence of the efficiency is not corrected in their result [23]. Considering that all of the measurements after applying our normalization agree with each other within our 10% systematic uncertainty, we expect the systematic uncertainties of the efficiency curves in the other measurements to be comparable to ours at $E_\alpha < 1.2$ MeV. A new measurement of $^{13}\mathrm{C}(\alpha,n)^{16}\mathrm{O}$ reaction cross section in the range of $E_\alpha = 4$–5 MeV is about 15% lower than the ENDF/B-VIII.0 evaluation [6]. This larger discrepancy suggests an even larger systematic uncertainty at higher energy. A new measurement within this energy region is needed to resolve the discrepancy.

The target thickness in the thin target measurements [3–5] is another important source of systematic uncertainty. For example, the target thickness of Harissopulos's measurement was suspected to be 30% smaller than the published value [3,8], leading to a normalization factor of 1.36. But such a problem does not exist in the thick target measurements [1,7,10]. At energies below $E_\alpha \approx 1.5$ MeV, the cross section and hence the thick target yield strongly depends on the beam energy. Consequently, a precise energy calibration is needed to provide a reliable reference for the normalization. As the maximum thick target yield $Y_{\max}$ of the resonant component does not depend on the beam energy, it offers a great opportunity to establish a standard yield to check the detection efficiency.

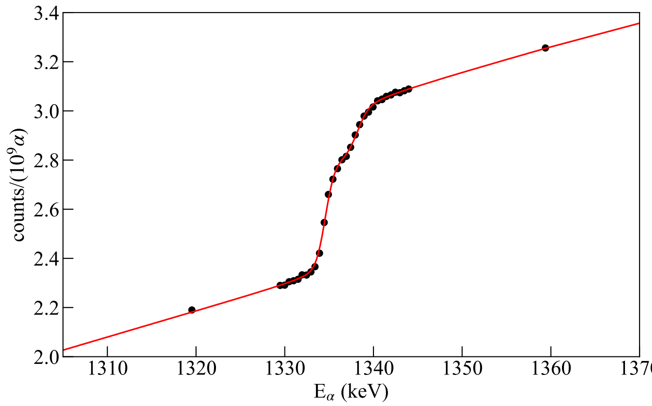

FIG. 5. Measured(black points) and fitted(red line) thick target yield near the $E_\alpha = 1336$ keV.

Two resonances are located at $E_\alpha = 1334.68$ and 1338.78 keV, respectively [9]. Thick target yields near these two resonances were measured as well. They are shown as black points together with our best fit in Fig. 5. Two resonances were extracted at 1334.64 ± 0.26 and 1338.27 ± 0.78 keV. As the two resonances are so close, the extracted strengths of the two resonances are strongly correlated, resulting in large uncertainties. By summing the two resonance strengths together, we obtain the sum of the two resonance strengths as $57.3 \pm 4.8(\mathrm{stat}) \pm 5.7(\mathrm{sys})$ eV. The systematic uncertainty includes the contributions from the beam current integration (5%), the stopping power (5%) and detection efficiency (7%) [14]. Our result is compared to other measurements in Table IV. The corresponding thick target yield is $Y_{\max} = 18.6 \pm 1.6(\mathrm{stat}) \pm 1.6(\mathrm{sys}) \times 10^4$ counts/(particle μC) in the condition of a pure ^{13}C sample and a detection efficiency of 100%. The systematic uncertainty is 8.6% as we discussed earlier in this paper.

In Bair and Haas's experiment, the sum of $\sigma_R\Gamma$ of the two resonances was reported to be 40.3 eV b (52.7 eV b in the

TABLE IV. Sum of the strengths of the resonances at $E_\alpha = 1334.64$ and 1338.27 keV.

Ref.	Resonance strength (eV)	Normalization
Bair *et al.*	48	1.19
Harissopulos *et al.*	33.3 ± 1.8	1.72 ± 0.24
This work	$57.3 \pm 4.8(\mathrm{stat}) \pm 5.7(\mathrm{sys})$	

laboratory frame) [7], corresponding to $\omega\gamma$ of 48.0 eV, without reported errors. The normalization factor is determined to be 0.95 ($= 1.19\times0.8$) with an uncertainty of $>10\%$, in good agreement with the normalization factor of 1.05(5), which is obtained from the strength of the narrow resonance at $E_\alpha = 1055.63$ keV. Harissopulos *et al.* reported a resonance strength of 33.3 ± 1.8 eV, leading to a normalization factor of 1.72(24), agreeing with our recommendation listed in Table III.

The lack of monoenergetic neutron source in the range of MeV introduces unknown systematic uncertainty in the measurement involving neutron detection. As we demonstrated earlier, rather large discrepancies exist among the measurements performed in the last half century. The present work demonstrates the importance and usefulness of the $^{13}C(\alpha, n)\,^{16}O$ reaction as a source for the semimonoenergetic neutrons in the ranges of 2.4 to 3.2 MeV and 2.5 to 3.5 MeV, which is critical for the calibration of neutron detection efficiency.

V. SUMMARY

The $^{13}C(\alpha, n)\,^{16}O$ reaction is an important reaction in stellar evolution, the geoneutrino experiments, and the criticality safety of nuclear reactors. It is also useful in the efficiency calibration of neutron detector arrays. However, the precision of the reaction cross section is limited by the inconsistency among the existing measurements. We performed a thick target yield measurement around the narrow resonance at $E_\alpha = 1055.63$ keV. The strength of the narrow resonance is determined to be $16.9 \pm 0.4(\text{stat}) \pm 1.7(\text{sys})$ eV. The resonance strength and the cross section in the vicinity of the resonance are used to reconcile the inconsistencies of the past measurements. Our normalization factors agree with the recommendation of the ENDF/B-VIII.0 evaluation and the CIELO project. The sum of the resonance strengths of the two narrow resonances around $E_\alpha = 1336$ keV is also determined to be $57.3 \pm 4.8(\text{stat}) \pm 5.7(\text{sys})$ eV. The thick target yields reported here are useful for the validation of the efficiencies of neutron detector arrays in the ranges of 2.4 to 3.2 MeV and 2.5 to 3.5 MeV.

ACKNOWLEDGMENTS

The authors would like to thank Prof. H.Y. Wu at Peking University for his help in the data acquisition software during the experiment. This work was supported by the Strategic Priority Research Program of the Chinese Academy of Sciences (No. XDB34020200) and National Natural Science Foundation of China under Grants No.11490564, No. 11805138, No. 12175156, and No. 11875329.

[1] B. Gao, T. Jiao, Y. Li, H. Chen, W. Lin, Z. An, L. Ru, Z. Zhang, X. Tang, X. Wang, N. Zhang, X. Fang, D. Xie, Y. Fan, L. Ma, X. Zhang, F. Bai, P. Wang, Y. Fan, G. Liu *et al.*, Phys. Rev. Lett. **129**, 132701 (2022).

[2] G. F. Ciani, L. Csedreki, D. Rapagnani, M. Aliotta, J. Balibrea-Correa, F. Barile, D. Bemmerer, A. Best, A. Boeltzig, C. Broggini, C. G. Bruno, A. Caciolli, F. Cavanna, T. Chillery, P. Colombetti, P. Corvisiero, S. Cristallo, T. Davinson, R. Depalo, A. DiLeva *et al.*, Phys. Rev. Lett. **127**, 152701 (2021).

[3] S. Harissopulos, H. W. Becker, J. W. Hammer, A. Lagoyannis, C. Rolfs, and F. Strieder, Phys. Rev. C **72**, 062801(R) (2005).

[4] M. Heil, R. Detwiler, R. E. Azuma, A. Couture, J. Daly, J. Görres, F. Käppeler, R. Reifarth, P. Tischhauser, C. Ugalde, and M. Wiescher, Phys. Rev. C **78**, 025803 (2008).

[5] H. W. Drotleff, A. Denker, H. Knee, M. Soine, G. Wolf, J. W. Hammer, U. Greife, C. Rolfs, and H. P. Trautvetter, Astrophys. J. **414**, 735 (1993).

[6] M. Febbraro, R. J. deBoer, S. D. Pain, R. Toomey, F. D. Becchetti, A. Boeltzig, Y. Chen, K. A. Chipps, M. Couder, K. L. Jones, E. Lamere, Q. Liu, S. Lyons, K. T. Macon, L. Morales, W. A. Peters, D. Robertson, B. C. Rasco, K. Smith, C. Seymour, G. Seymour, M. S. Smith, E. Stech, B. V. Kolk, and M. Wiescher, Phys. Rev. Lett. **125**, 062501 (2020).

[7] J. K. Bair and F. X. Haas, Phys. Rev. C **7**, 1356 (1973).

[8] M. Chadwick, R. Capote, A. Trkov, M. Herman, D. Brown, G. Hale, A. Kahler, P. Talou, A. Plompen, P. Schillebeeckx, M. Pigni, L. Leal, Y. Danon, A. Carlson, P. Romain, B. Morillon, E. Bauge, F.-J. Hambsch, S. Kopecky, G. Giorginis *et al.*, Nucl. Data Sheets **148**, 189 (2018).

[9] National Nuclear Data Center, https://www.nndc.bnl.gov/.

[10] C. R. Brune, I. Licot, and R. W. Kavanagh, Phys. Rev. C **48**, 3119 (1993).

[11] J. Pereira, P. Hosmer, G. Lorusso, P. Santi, A. Couture, J. Daly, M. D. Santo, T. Elliot, J. Görres, C. Herlitzius, K.-L. Kratz, L. Lamm, H. Lee, F. Montes, M. Ouellette, E. Pellegrini, P. Reeder, H. Schatz, F. Schertz, L. Schnorrenberger *et al.*, Nucl. Instrum. Methods Phys. Res. Sect. A **618**, 275 (2010).

[12] K. Brandenburg, G. Hamad, Z. Meisel, C. Brune, D. Carter, T. Danley, J. Derkin, Y. Jones-Alberty, B. Kenady, T. Massey, S. Paneru, M. Saxena, D. Soltesz, S. Subedi, and J. Warren, J. Instrum. **17**, P05004 (2022).

[13] J. Han, Z. An, G. Zheng, F. Bai, Z. Li, P. Wang, X. Liao, M. Liu, S. Chen, M. Song, and J. Zhang, Nucl. Instrum. Methods Phys. Res. Sect. B **418**, 68 (2018).

[14] Y.-T. Li, W.-P. Lin, B.-S. Gao, H. Chen, H. Huang, Y. Huang, T.-Y. Jiao, K.-A. Li, X.-D. Tang, X.-Y. Wang, X. Fang, H.-X. Huang, J. Ren, L.-H. Ru, X.-C. Ruan, N.-T. Zhang, and Z.-C. Zhang, Nucl. Sci. Technol. **33**, 41 (2022).

[15] D. Brown, M. Chadwick, R. Capote, A. Kahler, A. Trkov, M. Herman, A. Sonzogni, Y. Danon, A. Carlson, M. Dunn, D. Smith, G. Hale, G. Arbanas, R. Arcilla, C. Bates, B. Beck, B. Becker, F. Brown, R. Casperson, J. Conlin *et al.*, Nucl. Data Sheets **148**, 1 (2018).

[16] C. R. Brune and R. W. Kavanagh, Phys. Rev. C **45**, 1382 (1992).

[17] J. F. Ziegler, SRIM - the stopping and range of ions in matter, http://www.srim.org/.

[18] Stopping power and range tables for helium ions, National Institute of Standards and Technology (NIST), Physical Meas.

Laboratory ASTAR database, https://physics.nist.gov/PhysRefData/Star/Text/ASTAR.html.
[19] M. T. Pigni and S. Croft, Phys. Rev. C **102**, 014618 (2020).
[20] J. K. Bair, Nucl. Sci. Eng. **51**, 83 (1973).
[21] R. L. Macklin and J. H. Gibbons, Nucl. Sci. Eng. **31**, 343 (1968).
[22] R. Macklin, Nucl. Instrum. **1**, 335 (1957).
[23] J. K. Bair and J. G. del Campo, Nucl. Sci. Eng. **71**, 18 (1979).